Trimerization of Ethyne: Growth and Evolution of Ring Currents in the Formation of the Benzene Ring

Remco W. A. Havenith,[†] Patrick W. Fowler,*[,†] Leonardus W. Jenneskens,*[,‡] and Erich Steiner[†]

School of Chemistry, University of Exeter, Stocker Road, Exeter EX4 4QD, United Kingdom, and Debye Institute, Department of Physical Organic Chemistry, Utrecht University, Padualaan 8, 3584 CH Utrecht, The Netherlands

Received: October 22, 2002; In Final Form: January 20, 2003

Current density maps computed with the ipsocentric-distributed gauge ab initio CTOCD-DZ method and subjected to orbital-by-orbital analysis are used to follow the changing roles of σ and π electrons along the reaction coordinate for the trimerization of ethyne (**2**) to form benzene (**1**). The transition state (TS) is seen to sustain a diatropic-induced ring current that is entirely an induced circulation of the σ electrons; there is no sign of the benzenoid π current in the TS. On the downhill portion of the reaction path, the first change in the maps is that the inner part of the delocalized σ circulation is replaced by a central paratropic σ current as the new σ bonds relocalize. Only in the final stage of the reaction path does the typical benzenoid diatropic π ring current grow in. This sequence of changes from a σ-dominated to a π-dominated ring current accompanies the change of character of the highest occupied molecular orbital−lowest unoccupied molecular orbital gap from σ to π.

Introduction

The existence of a diatropic π ring current in a monocyclic system is taken as an unambiguous signature of aromaticity.[1] Ample evidence correlates the presence of diatropic and paratropic currents in planar or planarized monocycles with π electron counts of $4n + 2$ and $4n$, respectively.[2] A widely used local probe for these currents is NICS—the nucleus-independent chemical shift—at or near the ring center.[3,4] More directly, visualization of ring currents via current density maps is now computationally feasible[5−7] and has been used to build a physically based orbital model of the magnetic response of ground state π systems.[8,9]

Thermally allowed pericyclic reactions are considered to take place via a concerted pathway that passes through a $(4n + 2)$ electron transition state (TS) that is usually designated as "aromatic".[10,11] A well-studied example is the trimerization of ethyne (**2**) to form benzene (**1**, Chart 1).[12−16] The implication is that the TSs in such reactions should support diatropic ring currents,[12] and many previous theoretical studies using various magnetic criteria (^{1}H NMR chemical shifts, exaltation of diamagnetizability ($\Delta\chi$)) are in line with this expectation.[17−22] However, there is a continuing debate on the relative contributions made by σ and π electrons to the current in the TS of the ethyne trimerization.[12,23,24] Jiao and Schleyer concluded from a dissected NICS study that both σ and π electrons made significant contributions to a diatropic ring current in the transition state (NICS(σ) 56% and NICS(π) 44% of NICS(total)),[12] whereas for the same reaction, Morao and Cossío found from a study of the height profile of NICS values that there was no π aromaticity in the TS.[23]

CHART 1. Trimerization of Ethyne (2) to Benzene (1)

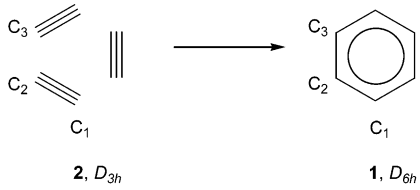

The most direct way to deal with this dichotomy would appear to be a computation of the ring currents themselves. In the present paper, we use an ipsocentric-distributed gauge ab initio method to visualize the evolution of the currents at different stages of this archetypal pericyclic reaction. Maps of σ, π, and individual orbital contributions to the induced current density are used to follow the changing roles of σ and π electrons along the reaction coordinate and to record the emergence of the characteristic magnetic features of benzene (**1**). As will be described below, the maps show a sequence of distinct stages in which the system is transformed from the localized σ and π circulations of the three discrete ethyne (**2**) monomers, through a TS with only a global σ ring current, to the well-known delocalized π circulation of benzene (**1**) itself.

Results and Discussion

As the trimerization of ethyne (**2**) to benzene (**1**) is symmetry-allowed according to the Woodward and Hoffmann rules,[10] a one-determinant wave function should be sufficient for the description of the essential features of this process. At the RHF/6-31G** level of theory, the TS for the trimerization has D_{3h} symmetry, with a single imaginary frequency (-1063 cm^{-1}) and carbon−carbon separations of 1.217 and 2.214 Å (see Supporting Information), in general agreement with previously reported results.[13−16] A similar D_{3h} TS is obtained at the RHF/6-31G* and MP2/6-31G* levels of theory, albeit with several

* To whom correspondence should be addressed. P.W.F.: Fax: +44-1392-263434. E-mail: P.W.Fowler@exeter.ac.uk. L.W.J.: Fax: +31-30-2534533. E-mail: jennesk@chem.uu.nl.
† University of Exeter.
‡ Utrecht University.

10.1021/jp0222907 CCC: $25.00
Published on Web 02/27/2003

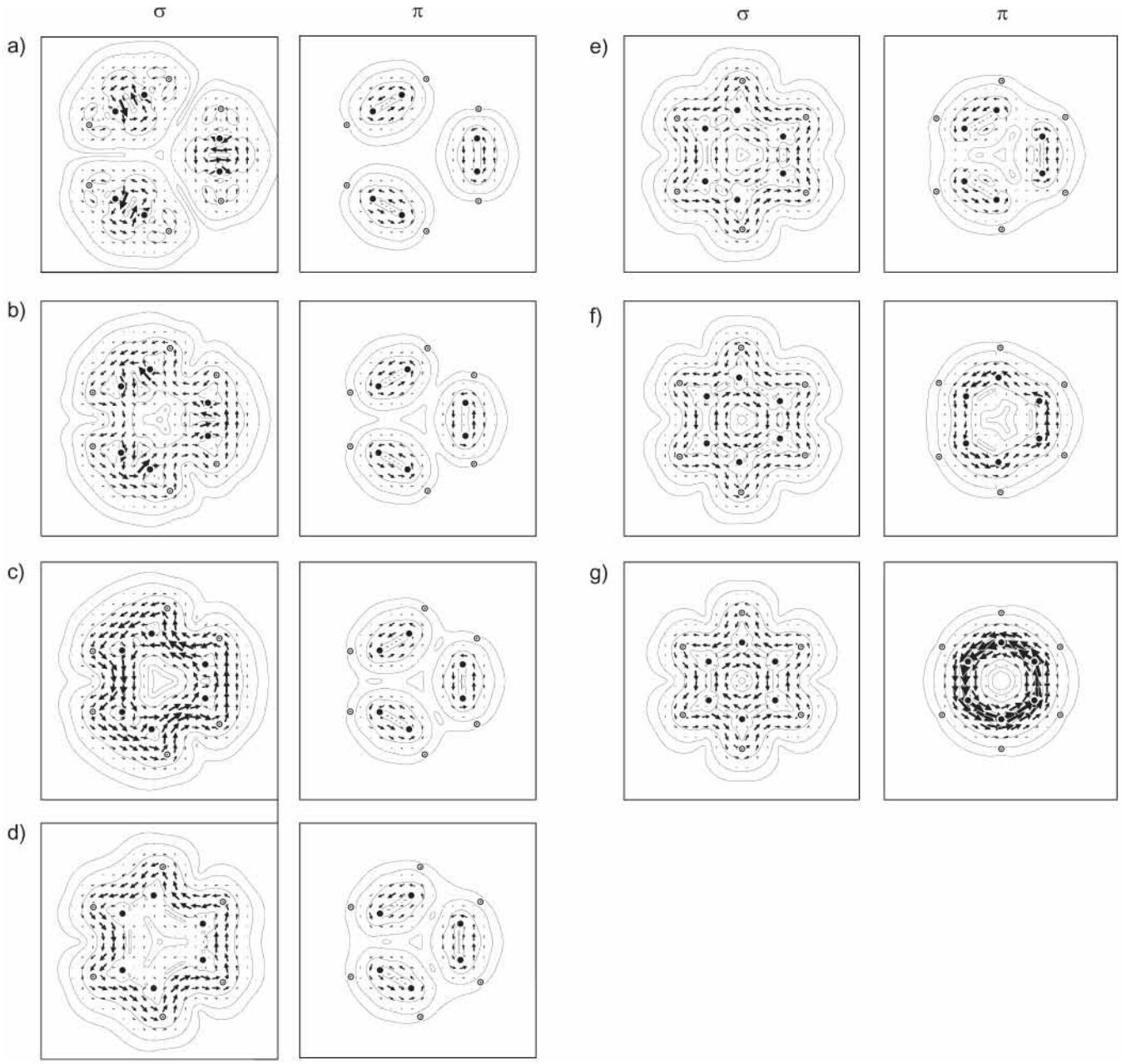

Figure 1. Maps of σ and π current density, induced by a unit magnetic field along the principal axis, plotted in a plane $1a_0$ above the molecular plane, at selected points on the reaction coordinate. (a) IRC = −1; $R(C_1-C_2)$ = 1.185 Å; $R(C_2\cdots C_3)$ = 3.119 Å (**2**). (b) IRC = −0.1; $R(C_1-C_2)$ = 1.194 Å; $R(C_2\cdots C_3)$ = 2.387 Å. (c) IRC = 0 (TS); $R(C_1-C_2)$ = 1.217 Å; $R(C_2\cdots C_3)$ = 2.214 Å. (d) IRC = 0.2; $R(C_1-C_2)$ = 1.292 Å; $R(C_2\cdots C_3)$ = 2.033 Å. (e) IRC = 0.4; $R(C_1-C_2)$ = 1.329 Å; $R(C_2\cdots C_3)$ = 1.907 Å. (f) IRC = 0.6; $R(C_1-C_2)$ = 1.358 Å; $R(C_2-C_3)$ = 1.697 Å. (g) IRC = 1; $R(C_1-C_2)$ = 1.386 Å; $R(C_2-C_3)$ = 1.386 Å (**1**).

low-frequency distortion modes at the MP2 level (e.g., a degenerate mode at 29 cm^{-1}).[25] At the MP2/6-311G** level, the change of basis is sufficient to convert the D_{3h} structure to a stationary point of higher order (with three imaginary frequencies[15]). In density functional theory (DFT) calculations, the D_{3h} structure remains a true TS at BLYP/6-311G** and B3LYP/6-311+G** levels.[12] Although the question of the precise symmetry of the TS is clearly a delicate one, the optimized bond lengths are insensitive to the "negligibly small"[15] changes in energy on distortion. Therefore, the current density maps are not expected to change appreciably with these distortions, and in fact, none of the arguments used in the present paper will depend critically on the precise symmetry of the TS.

Intrinsic reaction coordinate (IRC) calculations with GAMESS-UK[26] were performed to obtain geometries at a sequence of points on the reaction path (see Supporting Information). D_{3h} symmetry is found to be maintained along the reaction path. The structure with carbon−carbon distances of 1.185 and 3.119 Å is the endpoint of the search in the direction of reactants (three ethynes (**2**)) and is taken to have IRC = −1; the TS has by definition IRC = 0, and the equilibrium structure of benzene (**1**, with bond lengths of 1.386 Å in RHF/6-31G**) is the point with IRC = 1. In all, 150 geometries on the reaction path from IRC = −1 up to the TS and 98 geometries from the TS down to benzene were calculated. Current densities were computed at each geometry with the ipsocentric CTOCD-DZ formulation of coupled Hartree−Fock theory, using the SYSMO[27] program in the 6-31G** basis. In the selection of maps presented here, the current density is that induced by an external magnetic field acting at right angles to the plane of the nuclei. The plotting plane lies $1a_0$ above that of the nuclei. If plotted in the molecular plane, the σ current density near the nuclei would be complicated

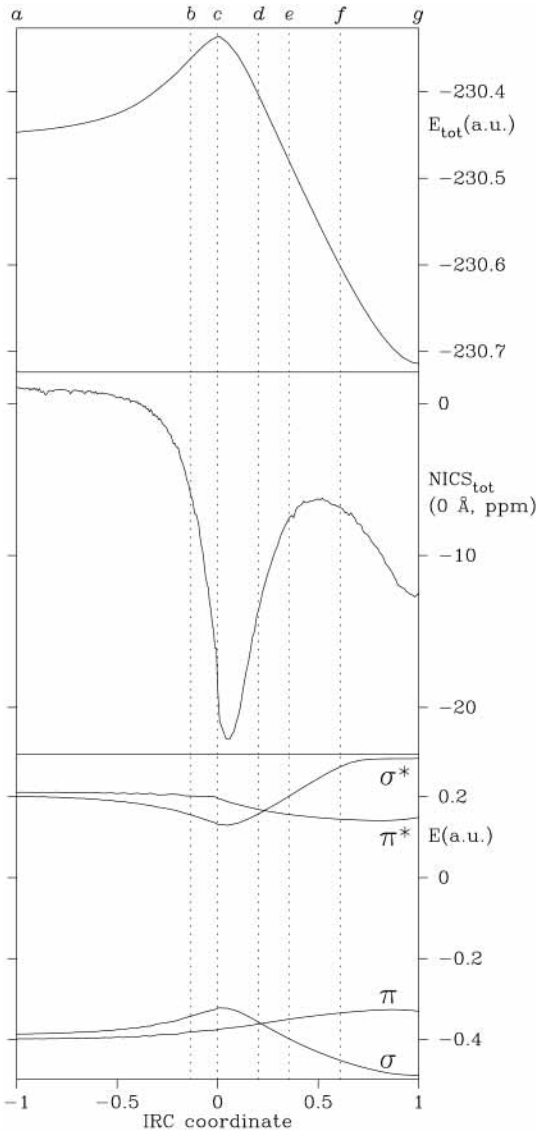

Figure 2. Total energy, NICS(0), and the orbital energies of the occupied 6e′ (σ), 1e″ (π) and unoccupied 7e′ (σ*), 2e″ (π*) orbitals as a function of the IRC coordinate. Indicated with dotted lines are the seven selected points for which the current density maps are shown (see Figure 1).

by strong local circulations, which are no longer visible at the height of $1a_0$. The contours show the modulus of the current density, and the vectors represent the in-plane projection of the current. In all plots, diamagnetic circulation is shown anticlockwise and paratropic circulation is shown clockwise.

Figure 1 shows σ and π current density maps at seven points, selected to illustrate the main stages along the reaction path: σ and π are here defined with respect to the molecular plane and thus, in addition to the axial sp−sp bonding orbitals of the ethyne fragments, the σ manifold includes those orbitals that at the earliest stage of the reaction are in-plane tangential p−p bonding orbitals on the fragments and hence are initially degenerate with some of the π orbitals.

At the beginning of the reaction path, where the system consists of three noninteracting ethyne molecules **2**, only localized currents are discernible (Figure 1a). As the molecules approach, the in-plane p orbitals start to interact, and a delocalized σ current starts to flow between them (IRC = −0.1; Figure 1b). From this point on the IRC, as the reaction moves toward the TS, we see the growth of a delocalized, fully diamagnetic, σ circulation on both the perimeter and the interior of the carbon framework, while the π currents remain essentially unchanged, as localized circulations around the short carbon−carbon bonds. In the TS (IRC = 0; Figure 1c) there is still no indication of a π ring current. On the downhill portion of the IRC, we see first the disappearance of the central part of the diatropic σ current and its replacement by a central paratropic σ current (compare Figure 1d (IRC = 0.2) and e (IRC = 0.4)). The evolution of a post-TS paratropic σ current is consistent with a relocalization of the σ bonds, signaling the formation in the product of the new localized, σ carbon−carbon C_2-C_3 bonds. It is significant that the central paratropic σ current emerges in the current density maps at a computed geometry (IRC = 0.6 (Figure 1f)), where the value of $R(C_2-C_3)$ (1.697 Å) is close to that found for the longest known sp^3-sp^3 carbon−carbon σ bond (1.78 Å).[28] Following this relocalization of σ electrons, the typical benzenoid diatropic π ring current starts to grow in (Figure 1e,f). This π current reaches full strength in the reaction product benzene (**1**; Figure 1g).

A recurring theme in previous studies of benzene has been the robustness of the π ring current (and hence aromaticity) of the benzene ring. Attachment of unsaturated clamping groups can effectively destroy the ring current, but this has been shown to be a result of electronic perturbation rather than a simple consequence of enforced bond alternation.[7b,29] The emergence of the π ring current on the reaction path at the first stage where the long contacts ($R(C_2-C_3)$[28]) could reasonably be called σ bonds is further evidence of the geometric tolerance and robustness of the archetypal benzene ring current.

Thus, the interpretation that emerges from the sequence of current density maps at $1a_0$ is that the D_{3h} 3 × C_2H_2 supermolecule sustains a diatropic ring current in the whole of the region of the IRC from the TS down to the product but that the character of this current changes continuously. A purely diatropic σ circulation in the TS gives way to weaker concentric paratropic and diatropic currents, which are then overshadowed by the strong diatropic π ring current of benzene (**1**).

These trends have implications for the integrated magnetic properties of the supermolecule. To compare our results with those of the previous NICS studies,[3,4,12,23] we evaluated the magnetic shielding at the ring center for all computed points on the reaction path, using the PZ2 variant of the CTOCD method.[30] The results are shown in Figure 2, which also includes information on the variation of the total and orbital energies along the reaction path. The calculated NICS profile (Figure 2b) is in good agreement with that reported by Jiao and Schleyer;[12] the total NICS (NICS(total)) value remains close to zero at the early stages of the reaction, decreases, reaches a minimum near the TS, and then increases again. The NICS property is an isotropic average, but its trend in this case is dominated by the strong contribution of the ring current to the out-of-plane shielding. With the post-TS onset of the paratropic σ current, the NICS value increases and then decreases as the π current strengthens. The complete domination of σ over π ring currents in the TS is however not evident in the isotropic NICS(0) property. Apparently, in this case, the height profile of the NICS value is a more reliable indicator of the minor role of the π electrons in the current at the TS.[23] Note that dissection of NICS(total) into NICS(σ) and NICS(π) has been performed, and it gave a ratio of σ:π contributions of 56:44.[4,12] However, the dissected NICS(σ) and NICS(π) quantities are still averages of the diamagnetism of the electron cloud under perturbation by magnetic fields in all directions. Ring current, per se, is solely the response to a magnetic field perpendicular to the molecular plane, and in the case of the present TS, this is a pure σ effect.

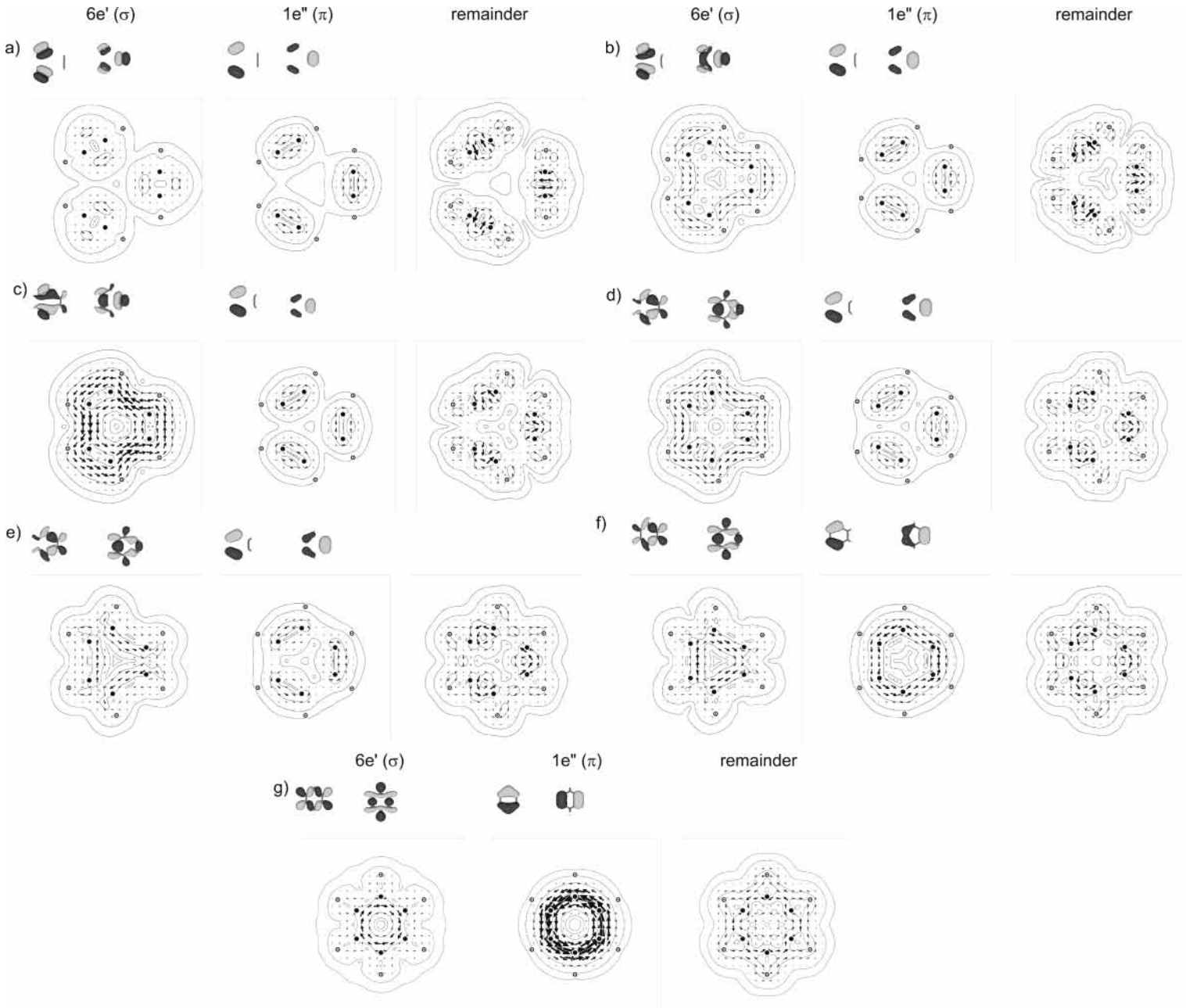

Figure 3. Orbital contributions from the 6e′, 1e″ orbitals to the total ($\sigma + \pi$) current density and the remaining part for the selected IRC points (see Figure 1).

Further insight into the nature of the induced current density can be gained by making an orbital-by-orbital analysis.[8] In an ipsocentric formulation, the orbital contributions arise naturally as sums over occupied-to-unoccupied transitions and are usually dominated by low-energy excitations of frontier electrons. Figure 3 shows the changing contributions of the highest occupied σ and highest occupied π orbital pairs to the current density map at the seven selected IRC points along the reaction coordinate. At each point, the specific contributions of electrons in these orbitals are compared with the current density arising from all of the remaining electrons.

The energies of the corresponding orbitals are shown as functions of the IRC in Figure 2c. For the early part of the IRC, from reactants to beyond the TS, the highest occupied molecular orbital (HOMO) of the system is of σ character and matched by a σ^* lowest unoccupied molecular orbital (LUMO). In the later stages of the reaction, π and π^* pairs take over as HOMO and LUMO. These energy changes have clear counterparts in the orbital current density maps of Figure 3. At the start of the reaction (Figure 3a), the current density in the plotting plane is localized and arises from the whole set of occupied valence orbitals. When the delocalized σ current begins to flow (Figure 3b), the contribution of the σ HOMO becomes more pronounced. At the TS (Figure 3c), the system can be described as four electron diatropic in the terminology of ref 8, and the dominant virtual excitation is the translationally allowed $\sigma \rightarrow \sigma^*$ HOMO−LUMO transition.[9] Then, as the reaction proceeds downhill from the TS, other $\sigma \rightarrow \sigma^*$ virtual excitations increase in relative importance. The combination of translationally and rotationally allowed transitions gives rise to the mixed outer diatropic and inner paratropic pattern that is to be expected of a cycle of localized bonds.[31] By the end of the reaction, the contribution from the highest σ orbital pair has become paratropic and can be identified with the paratropic current at the center of the benzene ring (Figure 3g).

A significant π ring current appears only in the downhill stage of the reaction, and as Figure 3e−g shows, it is always dominated by the π HOMO pair. The system remains four electron diatropic in the language of ref 8 at all stages, although now the electrons producing the current are in π and not σ orbitals. This ring current change from a σ-dominated to a π-dominated current is concomitant with the change of character of the HOMO−LUMO gap from σ to π.

Conclusion

Mapping of σ and π current densities has been found previously to be a useful tool in the study of systems at their equilibrium geometries. Here, it has been shown that these maps also have a useful application to the understanding of reacting systems. The maps, and their dissection into orbital contributions, make it possible to follow the evolution of the ring currents during the course of the formation of the benzene ring. The sequence of σ bond formation by initial delocalization and subsequent relocalization is accompanied by the appearance of a pure σ type ring current in the TS. The π ring current of benzene (**1**) appears late on the reaction pathway. Both features may be expected to hold for pericyclic reactions beyond the single example presented here.

Acknowledgment. We acknowledge a travel grant from the Royal Society of Chemistry (International Travel Grant 0012289; L.W.J.) and financial support from the European Union TMR Contract FMRX-CT097-0192 (BIOFULLERENES; R.W.A.H.).

Supporting Information Available: Total energies (E_{tot}, au; RHF/6-31G**) and Cartesian coordinates (RHF/6-31G**) of the IRC points. This material is available free of charge via the Internet at http://pubs.acs.org.

References and Notes

(1) For a review, see Schleyer, P. v. R.; Jiao, H. *Pure Appl. Chem.* **1996**, *68*, 209−218 and references therein.

(2) For recent reviews, see (a) Gomes, J. A. N. F.; Mallion, R. B. *Chem. Rev.* **2001**, *101*, 1349−1383 and references therein. (b) Lazzeretti, P. *Prog. Nucl. Magn. Reson. Spectrosc.* **2000**, *36*, 1−88 and references therein.

(3) Schleyer, R. v. P.; Maerker, C.; Dransfeld, A.; Jiao, H.; van Eikema Hommes, N. J. R. *J. Am. Chem. Soc.* **1996**, *118*, 6317−6318.

(4) Schleyer, P. v. R.; Manoharan, M.; Wang, Z.-X.; Kiran, B.; Jiao, H.; Puchta, R.; van Eikema Hommes, N. J. R. *Org. Lett.* **2001**, *3*, 2465−2468.

(5) Keith, T. A.; Bader, R. F. W. *Chem. Phys. Lett.* **1993**, *210*, 223−231.

(6) Coriani, S.; Lazzeretti, P.; Malagoli, M.; Zanasi, R. *Theor. Chim. Acta* **1994**, *89*, 181−192.

(7) (a) Steiner, E.; Fowler, P. W.; Jenneskens, L. W. *Angew. Chem., Int. Ed. Engl.* **2001**, *40*, 362−366. (b) Fowler, P. W.; Havenith, R. W. A.; Jenneskens, L. W.; Soncini, A.; Steiner, E. *Angew. Chem., Int. Ed. Engl.* **2002**, *41*, 1558−1560.

(8) Steiner, E.; Fowler, P. W. *J. Phys. Chem. A* **2001**, *105*, 9553−9562.

(9) Steiner, E.; Fowler, P. W. *Chem. Commun.* **2001**, 2220−2221.

(10) Woodward, R. B.; Hoffman, R. *The Conservation of Orbital Symmetry*; Verlag Chemie: Weinheim, 1970 and references therein.

(11) Zimmerman, H. E. *Acc. Chem. Res.* **1971**, *4*, 272−280 and references therein.

(12) Jiao, H.; Schleyer, P. v. R. *J. Phys. Org. Chem.* **1998**, *11*, 655−662.

(13) Houk, K. N.; Gandour, R. W.; Strozier, R. W.; Rondan, N. G.; Paquette, L. A. *J. Am. Chem. Soc.* **1979**, *101*, 6797−6802.

(14) Ioffe, A.; Shaik, S. *J. Chem. Soc., Perkin Trans. 2* **1992**, 2101−2108.

(15) Cioslowski, J.; Liu, G.; Moncrieff, D. *Chem. Phys. Lett.* **2000**, *316*, 536−540.

(16) Diercks, R.; Vollhardt, K. P. C. *J. Am. Chem. Soc.* **1986**, *108*, 3150−3152.

(17) Schleyer, P. v. R.; Jiao, H. *Angew. Chem., Int. Ed. Engl.* **1993**, *32*, 1763−1765.

(18) Schleyer, P. v. R.; Jiao, H. *J. Chem. Soc., Perkin Trans. 2* **1994**, 407−410.

(19) Herges, R.; Jiao, H.; Schleyer, P. v. R. *Angew. Chem., Int. Ed. Engl.* **1994**, *33*, 1376−1378.

(20) Jiao, H.; Schleyer, P. v. R. *Angew. Chem., Int. Ed. Engl.* **1995**, *34*, 334−337.

(21) Jiao, H.; Schleyer, P. v. R. *J. Chem. Soc., Faraday Trans.* **1994**, *90*, 1559−1567.

(22) Jiao, H.; Schleyer, P. v. R. *J. Am. Chem. Soc.* **1995**, *117*, 11529−11535.

(23) Morao, I.; Cossío, F. P. *J. Org. Chem.* **1999**, *64*, 1868−1874 and references therein.

(24) Bach, R. D.; Wolber, G. J.; Schlegel, H. B. *J. Am. Chem. Soc.* **1985**, *107*, 2837−2841.

(25) Wagenseller, P. E.; Birney, D. M.; Roy, D. *J. Org. Chem.* **1995**, *60*, 2853−2859.

(26) Guest, M. F.; van Lenthe, J. H.; Kendrick, J.; Schöffel, K.; Sherwood, P.; Harrison, R. J., GAMESS-UK, a package of ab initio programs, 2002; with contributions from Amos, R. D.; Buenker, R. J.; van Dam, H. J. J.; Dupuis, M.; Handy, N. C.; Hillier, I. H.; Knowles, P. J.; Bonacic-Koutecky, V.; von Niessen, W.; Harrison, R. J.; Rendell, A. P.; Saunders, V. R.; Stone, A. J.; Tozer, D. J.; de Vries, A. H. It is derived from the original GAMESS code due to Dupuis, M.; Spangler, D.; Wendolowski, J. *NRCC Software Catalog*, Program No. QG01; GAMESS: 1980; Vol. 1.

(27) Lazzeretti, P.; Zanasi, R. *SYSMO Package*; University of Modena: 1980. Additional routines for evaluation and plotting of current density: Steiner, E.; Fowler, P. W.

(28) (a) Fritz, G.; Wartanessian, S.; Matern, E. *Z. Anorg. Allg. Chem.* **1981**, *475*, 87−108. See also (b) Baldridge, K. K.; Kasahara, Y.; Ogawa, K.; Siegel, J. Y.; Tanaka, K.; Toda, F. *J. Am. Chem. Soc.* **1998**, *120*, 6167−6168 and references therein. (c) Bettinger, H. F.; Schleyer, R. v. P.; Schaefer, H. F., III. *Chem. Commun.* **1998**, 769−770 and references therein.

(29) (a) Fowler, P. W.; Havenith, R. W. A.; Jenneskens, L. W.; Soncini, A.; Steiner, E. *Chem. Commun.* **2001**, 2386−2387. (b) Soncini, A.; Havenith, R. W. A.; Fowler, P. W.; Jenneskens, L. W.; Steiner, E. *J. Org. Chem.* **2002**, *67*, 4753−4758.

(30) Zanasi, R.; Lazzeretti, P.; Malagoli, M.; Piccinini, F. *J. Chem. Phys.* **1995**, *102*, 7150−7157.

(31) Steiner, E.; Fowler, P. W. *Int. J. Quantum Chem.* **1996**, *60*, 609−616.